# Dynamic Response Analysis of Double-Line Ballast less Railway under Train

**WANG ZhongChang, DU XinMeng, LIANG Hongrui, ZHENG SHuai**

*Abstract*— **Under the condition of double-track parallel operation, the subgrade structure is subjected to the superimposed effects of intersecting train loads, resulting in complex dynamic response characteristics. Taking the subgrade engineering at the entrance of Limin Tunnel on the Harbin-Mudanjiang Passenger Dedicated Line as the research background, this study established a finite element model of the CRTS III slab ballastless track-subgrade-foundation structure using the ANSYS APDL module. Combining multi-body dynamics methods, the indirect coupling method was employed to analyze the dynamic responses of both the subgrade and track slab structures under train loading. The results indicate that stress concentration occurs at the interface between the subgrade and track slab. The vertical displacement time-history curves at different subgrade positions exhibit an initial increase followed by a decreasing trend, with vertical dynamic displacements forming a semi-elliptical distribution pattern under the track structure. The vibration-induced dynamic displacements in the subgrade attenuate along the depth direction and superimpose near the track centerline, reaching 1.26 mm vertical dynamic displacement at the subgrade base surface accompanied by 0.17 mm residual deformation. Particular attention should be paid to the soil strength at track slab edges and the central subgrade area. This research provides theoretical support for the design optimization and long-term service performance evaluation of double-track ballastless track subgrades.**

*Index Terms*—**train load; double-line ballasted track; finite element analysis; dynamic response; residual deformation**

## I. INTRODUCTION

With the continuous improvement of train running speed of high-speed railway[1-2], ballastless track has become the main track structure form of high-speed railway due to its advantages of high smoothness and low maintenance requirements. However, the dynamic load generated by train running at high speed is transmitted to subgrade through track structure, which may cause accumulated deformation, uneven settlement and dynamic instability of subgrade soil, which directly affects the service performance and running safety of railway line.

Many scholars use numerical simulation, field measurement, indoor test, theoretical analysis and other methods to study the dynamic response of track under train load. Zhai Wanming[3] established the train-track interaction model and took the lead in analyzing the vehicle-track vertical coupling dynamics. Shu Yao et al.[4], based on vehicle-track coupling dynamics theory, considered the vehicle body as a multi-rigid body system, vertically coupled the vehicle body and track system by Hertz nonlinear contact, established a ballastless track-vehicle vertical coupling dynamic model, and realized implicit fast solution of the dynamic model considering damage of foundation structure. Feng Jingchun et al.[5] established CRH3 train model based on multi-body dynamics software UniversalMechanism, considering the influence of track irregularity, and applied the wheel-rail vertical excitation load of train to finite element model through load subroutine. Liang Bo et al.[6-7] simplified the train body, and proposed an exciting force expression reflecting irregularity, additional dynamic load and rail surface wave wear effect to simulate train load from the formation reason of train vertical wheel-rail force. This method has clear definition and simple calculation, and has been widely used [8-9]. Zhang Lushun et al.[10] took the train load transfer law as the value reference in ballastless track design, established the train load analysis model, verified the model with indoor full-scale model, and proposed the relationship between ballastless track load transfer range and magnitude and dynamic coefficient. Chen Bojing et al.[11] established a three-dimensional dynamic model of train-turnout-ballastless track-viaduct bridge through ABAQUS software, and obtained the dynamic performance of track slab, vehicle and bridge when train passes. Shi Jin et al.[12] established a sleepers-ballast bed-piers-earth three-dimensional finite element model based on ANSYS software to calculate and analyze the influence of trains passing on viaducts on the subgrade of existing lines. Liu Gang et al.[13] studied the dynamic characteristics of ballastless track subgrade under train load by combining field monitoring, theoretical analysis and numerical simulation, and found that ballastless track slab can better diffuse train load to avoid local stress concentration, and the stress gradually attenuates along the depth direction, and the attenuation rate is 50% when it reaches the bottom of subgrade bed. Jiang Hongguang et al.[14] carried out experimental research on subgrade vibration characteristics and dynamic load transmission law under different train speeds based on full-scale high-speed railway slab ballastless track subgrade model test platform, and concluded that when the train speed exceeded 180km/h, the vibration speed of subgrade structure increased rapidly, and the gravel layer of subgrade structure could better absorb the vibration effect generated during train running. Existing researches focus on dynamic behavior of single track subgrade, but the dynamic

Manuscript received March 11, 2025

**WANG ZhongChang**, School of Transportation Engineering, Dalian Jiaotong University, Dalian , China.

**DU XinMeng**, School of Transportation Engineering, Dalian Jiaotong University, Dalian , China.

**LIANG Hongrui**, School of Transportation Engineering, Dalian Jiaotong University, Dalian , China。

**ZHENG SHuai**, School of Transportation Engineering, Dalian Jiaotong University, Dalian , China.

stress transfer mechanism, vibration energy distribution law and long term dynamic accumulation effect of subgrade under double track parallel condition are not fully understood. In this paper, the moving train load and its application method in finite element model are improved. The CRTS III slab double track ballastless track-subgrade-foundation structure model is established on the platform of finite element software ANSYS for calculation and secondary development. Combined with multi body dynamics method, The indirect coupling method is used to analyze the dynamic response of subgrade and track slab structure under train load, which is expected to provide scientific reference for subgrade engineering design of high-speed railway.

## II. Numerical Simulation of Train Load Process

### *A. Determination of ballastless track-subgrade-foundation structure model*

In this paper, the double-track ballastless track subgrade at the entrance of Limin Tunnel with the mileage of K68+786.09 on Harbin-Mudanjiang Passenger Dedicated Line is taken as the research object, and the CRTS III slab ballastless track-subgrade-foundation structure model of 1:1 is established by using the finite element software ANSYSAPDL module, as shown in Figure 1. Beam188 beam element is adopted to simulate rail element, Combin14 linear spring element is adopted to simulate fastener, longitudinal, transverse and vertical stiffness are respectively set as 15.12 kN/mm, 50 kN/mm and 35kN/mm to restrain rotation of lower end point of fastener spring. See Figure 2 for cross section of fastener. The track slab is 5.6m in length, 2.5m in width and 0.21m in thickness; the length of a single self-compacting concrete block is 5.6m, 2.5m in width and 0.1m in thickness; two bosses of 0.7m× 1m ×0.1m are set at the bottom as limit stops to improve the stability of the track slab, and the distance between the bosses is 2.8m. The length of the base plate is 5.6m, the width is 3.1m, and the height is 0.3m; two ends of the base plate are respectively provided with a groove, and the groove and the boss form a limiting structure. The slab gap between each two track slabs is 0.02mm, the total length of the model is 16.84m, the subgrade surface width is 13.6m, the height is 5.6m, the subgrade surface layer thickness is 0.4m, the filler is graded gravel, the subgrade bottom layer thickness is 2.3m, the filler is Group A and B, the embankment body thickness is 2.9m, the filler is gravel soil, and the subgrade slope gradient is 1: 1.5. The calculated width of the model is 64.8m, and the depth is 20m below the subgrade bottom surface. There are 4 layers of foundation soil in total. According to the engineering geological survey results, from top to bottom, there are respectively 1m thick silty clay layer, 3m thick fully weathered tuff, 7m thick strongly weathered tuff and 9m thick weakly weathered tuff.

The connection between track slab and self-compacting concrete adopts "door" type reinforcement, and it is assumed that the bonding between them is good in finite element model calculation, and the surface bonding is used for simulation. Geotextile is used as isolation layer for horizontal contact surface between self-compacting concrete and base slab, elastic rubber cushion is used as isolation layer between boss and groove, three-dimensional surface-to-surface contact Contac173 element is used for simulation of geotextile isolation layer in model, considering that its normal compressive stiffness is very large, it is considered that there is no normal relative deformation, hard contact is adopted, and friction coefficient is set to 0.7 in longitudinal and transverse directions according to actual data.

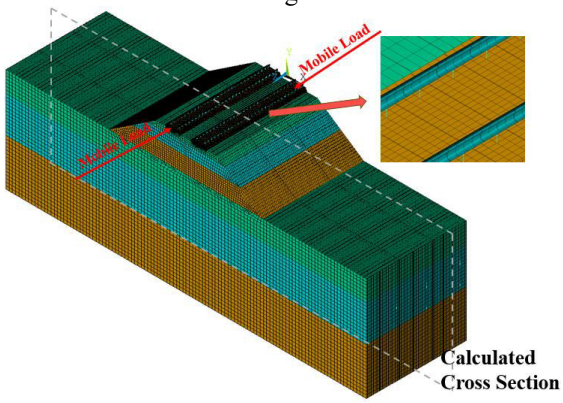


Fig. 1 Finite element model of CRTS III slab-type ballastless track-subgrade-foundation structure

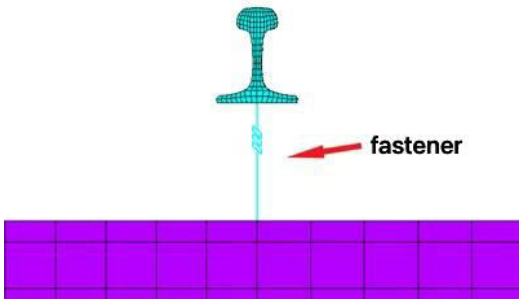


Fig.2 Cross-section of the fastener

The structural mechanical parameters of the ballasted track roadbed layers are shown in Table 1.

Table 1 Mechanical parameters of each structural layer in ballastless track subgrade

| Structure name | Modulus of elasticity/Gpa | Poisson's ratio | Densities /(kg·m$^{-3}$) | Angle of internal friction /(°) | Damping ratio |
|---|---|---|---|---|---|
| rail | 2.06×10$^{11}$ | 0.3 | 7850 | — | — |
| fastening | — | — | — | — | — |
| track board | 36 | 0.167 | 2500 | — | — |
| self-compacting concrete slab | 32.5 | 0.167 | 2450 | — | — |
| bed plate | 32.5 | 0.167 | 2500 | — | — |
| surface layer of subgrade bed | 190 | 0.27 | 2100 | 27 | 0.045 |
| bottom layer of subgrade bed | 110 | 0.25 | 2000 | 23 | 0.039 |
| embankment proper | 150 | 0.26 | 1900 | 20 | 0.035 |
| silty clay | 40 | 0.25 | 2000 | 18.1 | 0.08 |
| fully weathered tuff | 50 | 0.32 | 1830 | 28 | — |
| strongly weathered tuff | 51 | 0.26 | 2115 | — | — |
| weakly weathered tuff | 119 | 0.2 | 2400 | — | — |

*B. Realization of Train Load Simulation*

According to the finite element and vibration mechanics theory[15], the calculation model is discretized to obtain the dynamic equilibrium equations of each node in the motion state:

$$f_1 + f_D + f_S = p(t) \tag{1}$$

In the formula: $f_1$、$f_D$、$f_S$ and $p(t)$ are characteristic force vector, damping force vector, resistance force vector and external load vector. Equation (1) can be expressed as:

$$[M]\{\ddot{u}\} + [C]\{\dot{u}\} + [K]\{u\} = \{P\} \tag{2}$$

In the formula: M is the unit mass matrix, $M = \int_P N^T N d_\Omega$ ; $C$ is damping matrix, $C = \int_v N^T N d_\Omega$ ; $K$ is stiffness matrix, $K = \int B^T D B d_\Omega$ ; $P$ is nodal force load, $P = \int N^T b d_\Omega + \int N^T \overline{P} d_A$ ; $u, \dot{u}, \ddot{u}$ are nodal displacement, velocity and acceleration vectors respectively, $\dot{\mu} = \frac{\partial_u}{\partial_t}$ , $\ddot{\mu} = \frac{\partial_{u^2}}{\partial_{t^2}}$ ; $N$ is unit interpolation function; $\rho$, $v$ is material density and damping coefficient; $B$ is element strain matrix; $D$ is material stiffness matrix.

It is difficult to obtain the damping matrix accurately in practical calculation. Therefore, Rayleigh linear combination method is adopted to calculate the damping assumption [16],and its formula is as follows:

$$[C] = \alpha[M] + \beta[K] \tag{3}$$

In the formula: $\alpha$ and $\beta$ are Rayleigh damping coefficient, which are related to the natural frequency of the structure and its corresponding damping ratio.

Because it is difficult to determine the relationship between structural frequency and damping ratio of different materials in practical engineering, Therefore, assuming that the damping ratio remains constant under different vibration modes, the relationship between Rayleigh damping coefficient $\alpha$ and $\beta$and structural frequency and damping ratio can be obtained:

$$\frac{\alpha}{2w} + \frac{\beta w}{2} = \xi \tag{4}$$

In the formula: A is the circular frequency of the natural vibration of the structure, $\omega = 2\pi f$, The unit is Hz. $\xi$ is the damping ratio of the material.

In this paper, it is assumed that the natural frequencies of the models are consistent, and the natural frequencies of the first 10 orders of the model are taken, and the unified damping coefficient of the subgrade structure is calculated by combining the formula (4) $\alpha = 0.66$, $\beta = 0.001$.

It is assumed that the train is moving at a constant speed, and the train load is applied to the corresponding node of the rail in the form of moving dead load, so that the train load acts on the rail and moves along a certain direction with time. ANSYS uses Newmark implicit algorithm [17] to solve dynamic equations. Suppose that at times $t$ and $t + \Delta t$, the system accelerations are $\ddot{u}_t$ and $\ddot{u}_{t+\Delta t}$, displacement is $\Delta t$, then:

$$\dot{u}_{t+\Delta t} = \dot{u}_t + [(1-\alpha)\ddot{u}_t + \alpha\ddot{u}_{t+\Delta t}]\Delta t \tag{5}$$

$$u_{t+\Delta t} = u_t + \dot{u}_t \Delta t + [(0.5-\beta)\ddot{u}_t + \beta\ddot{u}_{t+\Delta t}]\Delta t^2 \tag{6}$$

Substituting the above two equations into equation (2), the equation of dynamic equilibrium for $t + \Delta t$ is:

$$[\overline{M}]\ddot{u}_{t+\Delta t} = [\overline{P}_{t+\Delta t}] \tag{7}$$

$$[\overline{M}] = [M] + [C]\alpha\Delta t + [K]\beta\Delta t^2 \tag{8}$$

$$\begin{aligned}[\overline{P}_{t+\Delta t}] = [P_{t+\Delta t}] - [C][\dot{u}_t + (1-\alpha)\ddot{u}_t\Delta t] \\ - [K][u_t + \dot{u}_t\Delta t + (0.5-\beta)\ddot{u}_t\Delta t^2]\end{aligned} \tag{9}$$

In the formula: $\alpha$ and $\beta$ are parameters of Newmark integration method; $[\overline{M}]$ is the equivalent mass matrix; $[\overline{P}_{t+\Delta t}]$—Equivalent load matrix.

Equation (9) gives $\ddot{u}_{t+\Delta t}$, By substituting equations (5) and (6), we can find out $\dot{u}_{t+\Delta t}$ and $u_{t+\Delta t}$。 However, in most cases, the finite element calculation system will seriously distort the higher-order vibration mode components caused by structural discretization. Therefore, Zienkiewica theory [18] is introduced to stipulate that Newmark implicit algorithm must satisfy the following requirements:

$$\begin{cases}\alpha \geq 0.5 \\ \beta \geq 0.25(0.5+\alpha)^2 \\ 0.5 + \alpha + \beta > 0\end{cases} \tag{10}$$

Where the Newmark parameters $\alpha$ and $\beta$ are entered according to the following formula:

$$\begin{cases}\alpha = 0.5 + \gamma \\ \beta = 0.25(1+\gamma)^2\end{cases} \tag{11}$$

In the formula: $\gamma$ is the amplitude attenuation factor.

From equations (10) and (11), it can be seen that Newmark algorithm can obtain stable solutions when $\gamma \geq 0$. In general, 0.005 is chosen. In this case, a smaller amplitude attenuation factor can eliminate the interference of higher mode shapes on the calculation results.

The Harbin-Mudanjiang Passenger Dedicated Line adopts CRH380B EMUs with a design speed of 250km/h and an 8-car formation in the form of "four motors and four trailers". It is the only one in my country that can operate normally in weather conditions ranging from 40℃ to 40℃. The whole train is 200.65m long, of which the length of the head and tail cars is 25.85m, and the length of the middle car is 24.825m. The axle weight is required to be less than 17t, and the static wheel weight of one side is 80kN. In this paper, the length of the model is three track plates, the total length is 16.84m, the train load when the middle car passes is selected, and each hub of a single car acts on a single rail node.

*C. Boundary conditions*

For the dynamic response of subgrade and foundation,

because of the restriction of finite element solver, it is impossible to approach the infinite domain under the actual condition by infinitely increasing the model size, which leads to the reflection of vibration wave at the boundary of the model and affects the calculation accuracy. In this paper, three dimensional uniform viscoelastic artificial boundary [19-20] is adopted, symmetrical constraints are imposed on the periphery of subgrade model, the bottom boundary is completely fixed, and the axial movement and lateral rotation are constrained at both ends of rail. To reduce the calculation error of the model.

*D. Model validation*

Beidou high-precision positioning technology (mainly including centimeter-level Beidou displacement monitoring terminal, deep displacement sensor, temperature sensor and soil moisture sensor) can directly reflect the instantaneous and long-term changes of horizontal displacement and elevation displacement of different active layers of subgrade structure[21]. The system is composed of data acquisition sensing, data transmission and host computer software. The error level of surface horizontal displacement monitoring is controlled within ±2.5mm+1ppm, and the elevation direction is ± 3mm +1ppm. The monitoring frequency is 60 times per minute. Figure 3 shows the numerical simulation and measured data curve of subgrade vertical displacement varying with time when two-way train passes by. It can be seen from the figure that vertical displacement increases first and then decreases with the passing of train, and tends to be stable after a period of time. The variation range of subgrade surface displacement in monitoring data is 1.25mm~ 0mm, and the variation range of subgrade surface displacement in model established in this paper is -1.17mm~0mm; The monitoring results verify the correctness of the numerical simulation method. Because the mechanical parameters of the same level take a single value in the numerical calculation process, and the influence of groundwater and temperature is not considered, and the uncertainty of the actual soil layer, groundwater and temperature makes the numerical analysis results slightly different from the measured results.

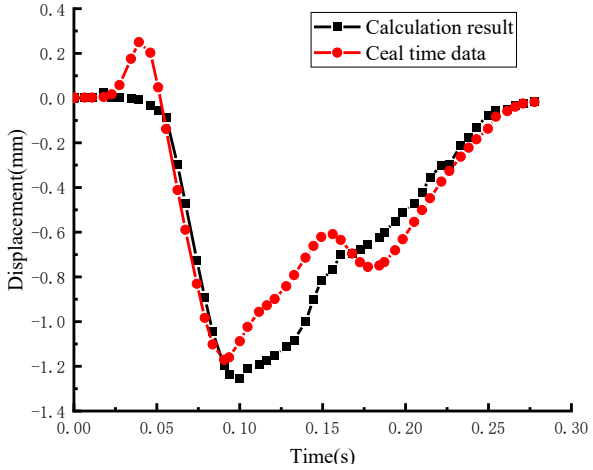


Fig.3 Comparison of measured and calculated results

## III. ANALYSIS OF NUMERICAL CALCULATION RESULTS

*A. Time History Analysis of Vertical Displacement and Stress of Subgrade*

Figure 4 shows the vertical stress and displacement time-history curves of nodes at different positions at z=8.42m under double-track train load. The train load is transferred from track structure to subgrade and foundation, and the stress and displacement of each structural layer attenuate along the depth direction. Two trains run opposite to each other and reach the center of track plate respectively at t=0.138s. The stress variation curve of track plate center presents symmetrical distribution, and the symmetry axis is the initial value of stress respectively. Because of the uneven distribution of load direction and position on both sides of subgrade center and the influence of stress transfer hysteresis, there is fluctuation near the initial stress value. The peak value of vertical displacement is reached at t=0.101s, which is 0.037s earlier than t=0.138s when train load arrives at this node. According to the train load passing through the same time and different positions, the stress and displacement changes at the center of the left track plate and the right track plate are basically the same due to the same train load directly, and the stress and displacement changes are more obvious than those at other positions. When the train runs through the model, there is residual deformation of 0.17mm in the center of subgrade, and the dynamic stress and displacement of subgrade surface have the same trend at different time, but the amplitude is slightly different, and the dynamic response amplitude is the largest at t=0.138s.

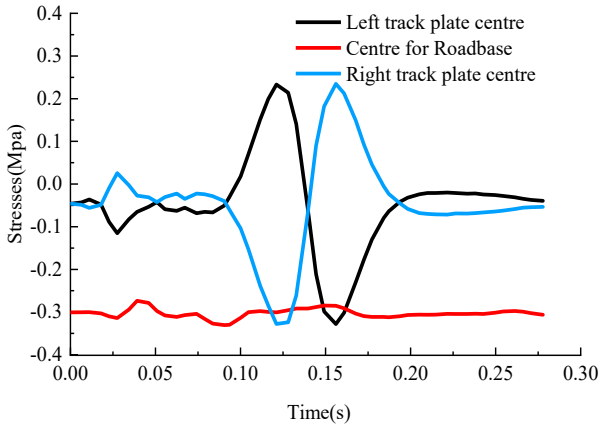


(a) Vertical dynamic stress

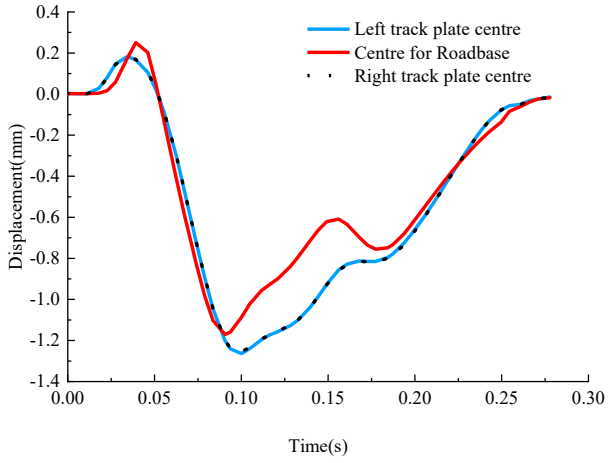


(b) Vertical displacement

*B. Analysis of time history of subgrade acceleration*

Figure 5 shows the acceleration time-history curves of nodes at different positions at z=8.42 m under double-track train load. It can be seen from the figure that the acceleration variation trend and value of the node at z=8.42 m in the center of left and right track slab are basically the same with time,

and the acceleration peak value is reached at t=0.023 s, t=0.034 s, t=0.051 s and t=0.100 s, which is 0.038s earlier than the time t=0.138s when the train load reaches this node. The acceleration peak value at the center of subgrade is larger than that at the center of track slab under double-track train load.

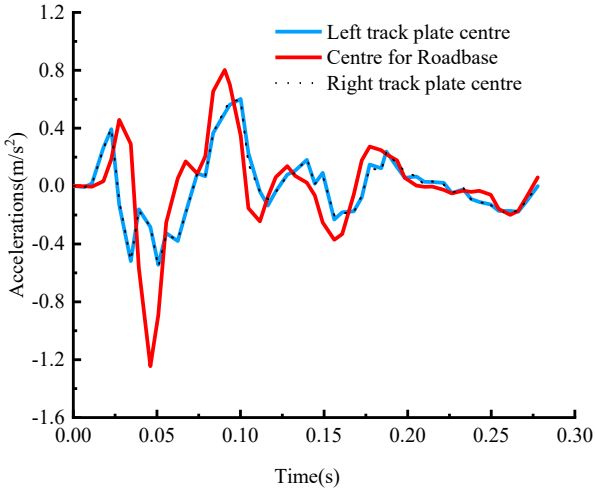


Fig. 5 Acceleration time-course curves of nodes at different locations of the roadbed at z=8.42m under two-lane train loading

The acceleration time-history data is transformed into frequency-amplitude data by fast Fourier method, as shown in Figure 6. It is found that the acceleration frequency generated by train with speed of 250km/h to the center of track slab has maximum amplitude at 10.596Hz, which is 0.198. Train load has great influence on subgrade acceleration frequency and amplitude.

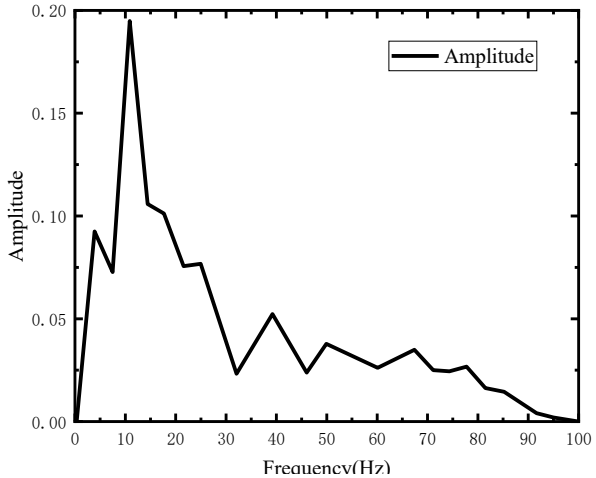


Fig.6 Frequency amplitude curve of the centre node of the left track slab at z=8.42m of the roadbed under double line train loading

### *C. Analysis of train load influence area*

The vertical displacement distribution of subgrade longitudinal section when the train load of double-track line moves to z=8.42m is shown in Figure 7. It can be seen from the figure that the load of double-track train mainly affects the left and right track plates and subgrade areas, and the vertical displacement distribution range is distributed in a symmetrical semi-elliptical shape along the centerline of the subgrade. The displacement of the left and right track plates directly acted by train load is the largest; with the increase of subgrade depth, the influence range of load on subgrade displacement becomes larger, but the displacement decreases gradually.

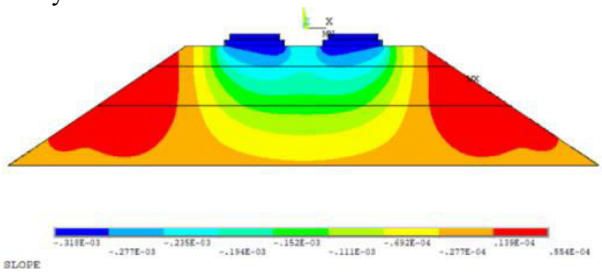

Fig. 7 Region of displacement change of longitudinal section of roadbed z=8.42m under double line train loading

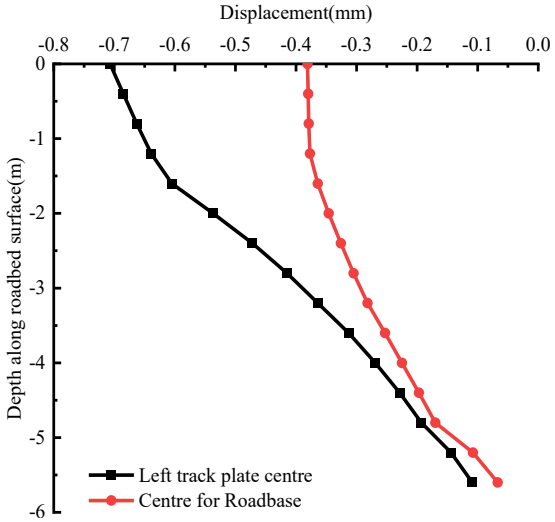


Fig. 8 Variation of displacement along the depth at different locations under double line train loading

Take the subgrade surface as 0m, and draw the vertical displacement variation curve of the center of left track slab and subgrade along the depth at z=8.42m under the load of double-track train, as shown in Figure 8. It can be seen from the figure that the vertical displacement of each position in different periods decreases gradually with the increase of depth, and the displacement change is basically 0 when it reaches the bottom of subgrade. The maximum displacement of subgrade surface is also 0.707mm under the center of track slab, and the maximum displacement of subgrade surface center is 0.381mm. Generally speaking, the displacement variation is less than 1mm, which will not affect the smooth operation of the train temporarily.

## IV. EPILOGUE

CRTS III slab ballastless track-subgrade-foundation structure model is established based on ANSYSA PDL module. Combined with multi-body dynamics method, indirect coupling method is adopted to analyze the dynamic response of subgrade and track slab structure after train load is applied. The following conclusions are obtained:

(1) Based on numerical model, the vertical dynamic displacement amplitude of subgrade under train speed is compared with the measured data to verify the validity and correctness of finite element model and moving train load application method.

(2) CRTS III slab ballastless track subgrade under double-track train load, the stress peak arrival time is slightly earlier than the train load; stress changes are symmetrical up and down, and the trend is just opposite.

(3) The maximum vertical displacement peak value of double-track train load is-1.26mm, which occurs on the

surface of track slab and produces residual deformation of 0.17mm. The vertical displacement decreases gradually with the increase of depth under train load, and the main influence depth is in the range of 0~5.6m from subgrade surface to subgrade bottom.

(4) When a train with a speed of 250m/s runs on this subgrade, the maximum amplitude of acceleration frequency generated by subgrade under double-track train load is 0.198 at 10.6 Hz. It can be found that train load has great influence on acceleration frequency and amplitude of subgrade. The strength of subgrade center area should be paid attention to in design.

## REFERENCES


[1] REN Nanqi, XU Zhicheng, LUYintao, et al.Thinking on Carbon Emission Characteristics and EmissionReduction Path in Railway Operation Period[J].Railway Standard Design, 2022, 66(7): 1-6.

[2] WEI Qiangwen, ZHU Shengyang, LUO Jun. Study on the Influence of Ballastless Tracks Interface Debonding on the Dynamic Properties of Vehicle-Track System in 400 km/h High-speed Railways[J].Railway Standard Design, 2023, 67(3):74-79.

[3] ZHAI Wanming. Vehicle-track coupling dynamics (third edition) [M]. Beijing: Science Press, 2007.

[4] SHU Yao, JIANG Zhongcheng, ZHANG Jun, et al.Dynamic Coupling Model of Ballastless track-vehicle Considering the Base Structural Damage and Its Solution[J]. Engineering Mechanics, 2021,38(3):181-191,213.

[5] FENG Jingchun, LUO Wenjun, XU Xinyang, et al. Study on Dynamic Displacement of Ballastless Track subgrade Under High-Speed Moving Load[J]. Journal of East China Jiaotong University, 2021, 38(4):45- 53,126.

[6] LIANG Bo, CAI Ying. Dynamic analysis on subgrade of high speed railways in geometric irregular condition[J].Journal of the China Railway Society, 1999(2):93-97.

[7] LIANG Bo, LUO Hong, SUN Changxin. Simulated Study on Vibration Load of High Speed Railway[J].Journal of the China Railway Society, 2006(4):89-94.

[8] XIE Q, WU Z H, DONG J, et al. Matrix Test Measurements of Ground-borne Vibration Induced by the Heavy-duty Trains on Embankment and Cutting Tracks in a Loess Area[J]. Earthquake Engineering and Engineering Vibration,2021,20(3):605-620.

[9] CHEN Zhifeng, LI Yingxiong, LAI Yuanming,et al.Non-stationary Random Vibration Analysis of Railway Embankments in Permafrost Regions under TrainLoads Using the Explicit Time-domain Method[J]. Journal of Glaciology and Geocryology, 2022, 44(2):555-565.

[10] ZHANG Lvshun, YU Lei, ZHAO Lei, et al. On the characteristics of static transfer of train load in double block ballastless track of high-speed railway [J]. Journal of Railway Science and Engineering, 2021, 18(8): 1951- 1959.

[11] CHEN Bojing, CAI Xiaopei,LI Chenghui, et al. Influence of bridge settlement on dynamic characteristics of ballastless turnouts[J]. Journal of Railway, 2013, 35(10): 100-105.

[12] SHI Jin, ZOU Kai, GU Aijun et al. Study on the impact of high-speed railway elevated line train operation on the roadbed of existing line[J]. Geotechnical Mechanics, 2013, 34(S2): 285-290.

[13] LIU Gang, LUO Qiang, ZHANG Liang et al. Analysis of dynamic stress characteristics of ballasted track roadbed under train loading[J]. Journal of Railway, 2013, 35(09): 86-93.

[14] JIANG Hongguang, BIAN Xucheng, XU Xiang et al. Full-scale physical model test of dynamic state of slab track roadbed of high-speed railway under moving train load[J]. Journal of Geotechnical Engineering, 2014, 36(2):354-362.

[15] WANG Xucheng,SHAO Min. Fundamental principles and numerical methods of the finite element method (second edition) [M]. Beijing: Tsinghua University Press, 1997.

[16] LI Peng. Dynamic Response and Long-term Cumulative Deformation Characteristics of Heavy Load Railway Roadbed [D]. Harbin Institute of Technology, 2018.

[17] BAO Chen, WANG Hu Jia. ANSYS engineering analysis advanced examples (revised edition) [M]. Beijing: China Water Resources and Hydropower Press, 2009: 105-168.

[18] Lankiewicz, Taylor. Fundamentals of the finite element method (Volume 1) [M]. Beijing: Tsinghua University Press, 2008: 69-84.

[19] CAO Yanmei, WANG Fuxing, ZHANG Yunshi. Research on the analysis method and characteristics of site vibration under the action of high-speed trains[J]. Journal of Railway, 2017, 39(6): 118-124.

[20] XUE Fuchun. Dynamic displacement analysis of track-roadbed of high-speed railway under moving load[J]. Journal of Earthquake Engineering, 2019, 41(5): 1105-1113.

[21] LIAN Hongjun, ZHANG Tao, YAN Xiaodong, ZHANG Tao, Wang Zhongchang. Analysis on deformation monitoring of high-speed railway tunnel entrance slope in seasonal freezing region[J]. Journal of Dalian Jiaotong University, 2023, 44(3): 85-91.